Iranian Journal of Remote Sensing & GIS. *2026, 18 (2): 143-174* P-ISSN: 2008-5966, E-ISSN: 2588-6185

Original Article

Hydro-Ecological Effects of Land-Use Change and Climate Variability: Insights from the Kashafrud River Basin, Northeastern Iran (1973–2023)

Mahshid Hosseini[1], Hossein Mostafavi[1*], Khosro Piri[1], Majid Delavar[2], Kamran Davari[3]

Affiliation

1. *Dep of Biodiversity and Ecosystem Management, Environmental Sciences Research Institute (ESRI), Shahid Beheshti University, Tehran, Iran.*
2. *Dep of Water Engineering and Management, Faculty of Agriculture, Tarbiat Modares University, Tehran, Iran.*
3. *Dep of Water Sciences and Engineering, Faculty of Agriculture, Ferdowsi University of Mashhad, Mashhad, Iran.*

ABSTRACT

This study assessed the combined impacts of climate variability and land-use change on the hydrological regime of the Kashafrud River Basin, Iran, during 1973–2023. Hydroclimatic data, statistical trend analyses, Google Earth Engine land-use mapping, and Indicators of Hydrologic Alteration (IHA) were applied to assess long-term changes. The results revealed a significant decline in precipitation, particularly in upstream areas, alongside a persistent increase in temperature throughout the basin. Land-use analysis showed substantial urban expansion and agricultural development over the five decades. These climatic and land-surface changes have jointly altered runoff generation, infiltration, evapotranspiration, and groundwater recharge processes. The river's natural flow regime has consequently been disrupted, as reflected by reduced low flows, shifts in peak-flow timing, and increased flow variability. The findings demonstrate that streamflow alterations result from the synergistic interaction of climatic changes and human-induced land-use transformations. Therefore, integrated and adaptive land and water management, conservation agriculture, and improved water governance are essential to enhance ecological integrity and water security in this semi-arid basin.

Keywords: Hydrologic Alteration, Trend Tests, Land-Use Change, Kashafrud River Basin, Water Resource Management.

* Corresponding Author: hmostafaviw@gmail.com
DOI: https://doi.org/10.48308/gisj.2026.244848.1352
Received: 2026.06.13
Accepted: 2026.07.13

Copyright: © 2026 by the authors. Submitted for possible open access publication under the terms and conditions of the Creative Commons Attribution (CC BY) license https://creativecommons.org/licenses/by/4.0/).

1. Introduction

Human and natural systems are closely interconnected through processes operating across spatial and temporal scales. The strong relationship among climate, water, and land use has raised increasing concern in recent decades (Dibaba et al. 2020). These interactions can have substantial environmental consequences, including biodiversity loss, hydrological change, land degradation, and lower agricultural productivity (Garg et al. 2019). Watershed hydrology is shaped by vegetation cover, soil properties, geology, climate, land-use practices, and the spatial organization of their interactions (Zhang et al. 2025), all of which can significantly influence streamflow, flood frequency, base flow, groundwater recharge, and mean annual discharge in river basins (Puno etal. 2019; Kumar et al. 2022). It is now widely recognized that these factors are strongly affected by human activities as well as climate change (Giglou et al. 2024). Consequently, understanding the interactions among climate, land use, and hydrological processes is essential for water resource management and for reducing the negative impacts of environmental change on watershed systems.

Climate change is widely recognized as a major driver of hydrological change because it intensifies the global water cycle and increases the frequency of extreme events, such as floods and droughts (Yan et al. 2016). These changes can affect both the quantity and quality of freshwater resources and alter hydrological processes, increasing the frequency and intensity of extreme events. Moreover, changes in precipitation and hydrological conditions can substantially affect ecosystems, agricultural production, and water availability (Bekele et al. 2019). Climate variability alters hydrological regimes by changing runoff timing, peak flow magnitude, and total flow volume (De Girolamo et al. 2022; Mekonnen et al. 2018). Furthermore, land use and climate regulate the basin's hydrological behavior through complex interactions across multiple spatial and temporal scales (Garg et al. 2019). Human-driven land use changes, such as urbanization and agricultural intensification, can significantly affect watershed hydrology by altering infiltration, surface runoff, and evapotranspiration processes (Kumar et al. 2022). These changes cause hydrological regime shifts and threaten water security and ecosystem stability, particularly in arid and semi-arid regions where water resources are already under stress.

Quantifying watershed hydrological responses is challenging because these responses are governed by complex interactions among topography, climate, and hydrological conditions. This makes it essential for land-use planners and water resource managers to identify and quantify such effects at the watershed scale. Several studies have examined the individual impacts of climate variability or land-use change on

hydrological processes (Xiong and Yang, 2024; Wang et al. 2014a, b; Niraula et al. 2015). However, fewer studies have investigated their combined influence at the watershed scale, despite its importance for a more complete understanding of hydrological responses (Mishra et al. 2009; Kim et al. 2013; Yin et al. 2017). Therefore, an integrated approach that simultaneously examines climatic variability and land-use dynamics is needed to better capture their synergistic effects on hydrological systems (Suryavanshi et al. 2017).

The Kashafrud River Basin (KRB), located in northeastern Iran, is an important hydrological and ecological region that supports agricultural activities, urban settlements, and industrial development (Gholizadeh Sarabi et al. 2021). Owing to its semi-arid climate and seasonal hydrological regime, the basin is highly sensitive to both climatic fluctuations and land-use transformations. In recent decades, population growth and economic development have led to significant changes in land cover, including expansion of built-up areas, reduction in vegetation cover, and changes in barren land and water bodies. Together with climate variability, these changes are likely to have altered streamflow patterns and water availability in the basin.

This study aimed to address this gap by providing a comprehensive assessment of the combined effects of climate variability and land use change on the hydrological regime of the KRB over the period 1973–2023. Specifically, this study: (1) examines long-term trends and abrupt changes in key hydro-climatic variables, including precipitation, temperature, and streamflow, using the Mann-Kendall test, Sen's slope estimator, and Pettitt's test; (2) quantifies the spatiotemporal dynamics of land use for 1973, 1983, 1993, 2003, 2013, and 2023 using the Google Earth Engine platform; and (3) evaluates the resulting changes in the river's flow regime through the Indicators of Hydrologic Alteration (IHA) framework. By integrating statistical trend analysis, remote sensing, and hydrological assessment tools, this study provides a basis for improved water resource management and offers insights for policymakers and environmental planners in semi-arid regions facing increasing environmental pressure. This study also highlights the value of multidisciplinary approaches for understanding the complex interactions among climate, land use, and hydrology in watershed management. Unlike previous studies in the KRB, which have mainly focused on isolated aspects of hydro-climatic variability or land-use dynamics, the present study provides an integrated long-term assessment of hydro-climatic change, land-use transformation, and hydrological alteration within a unified analytical framework. This study contributes to improving the understanding of how climate variability and land-use change collectively

influence streamflow characteristics and ecological flow conditions in semi-arid river basins. In addition, the integration of statistical trend analysis, remote sensing-based land-use evaluation, and the IHA framework offers a comprehensive approach that can support sustainable watershed and environmental flow management under increasing environmental stress.

2. Materials and Methods

Study Area

The KRB, located in northeastern Iran, and includes Mashhad, the country's second largest and most populous city. The basin has played an important role in the region due to the social, cultural, religious, and political development of Mashhad over time (Gholizadeh Sarabi et al. 2021). Covering approximately 16,500 km^2, the basin has an elevation range of 398 to 3224 m, with a mean elevation of 1496 m. The basin experiences a semi-arid climate with an average annual precipitation of approximately 236 mm.

Despite limited water availability and low precipitation, approximately 140,000 ha of irrigated agricultural land are used for food production in the basin, highlighting the importance of water resources for local livelihoods and development (Pareeth et al. 2019). The Kashafrud River flows from northwest to southeast through a canyon formed by the Hezar Masjed and Binalud Mountains before joining the Harirud River at the Iran-Turkmenistan border (Fig. 1).

Data Collection

This study used hydro-climatic and geospatial datasets to assess long-term environmental changes in the KRB. Hydro-climatic data, including daily streamflow and monthly precipitation and temperature records, were obtained from the Razavi Khorasan Regional Water Company (RKRWC). To ensure data consistency across the 50-year study period (1973–2023), linear and multiple regression methods were employed to fill gaps in stations with missing records.

Landsat imagery from 1973, 1983, 1993, 2003, 2013, and 2023 was used for land-use analysis. All imagery was processed using the Google Earth Engine (GEE) platform. A supervised classification approach based on the Random Forest algorithm was applied to classify the basin into four major land-use classes: water bodies, vegetation cover, built-up areas, and bare lands. A detailed summary of the datasets used in this study is presented in Table 1.

Analytical Methods

The analytical framework combined nonparametric trend analysis, abrupt change detection, remote sensing-based land-use mapping, and hydrological alteration assessment. Figure 2 shows the overall workflow used in this study.

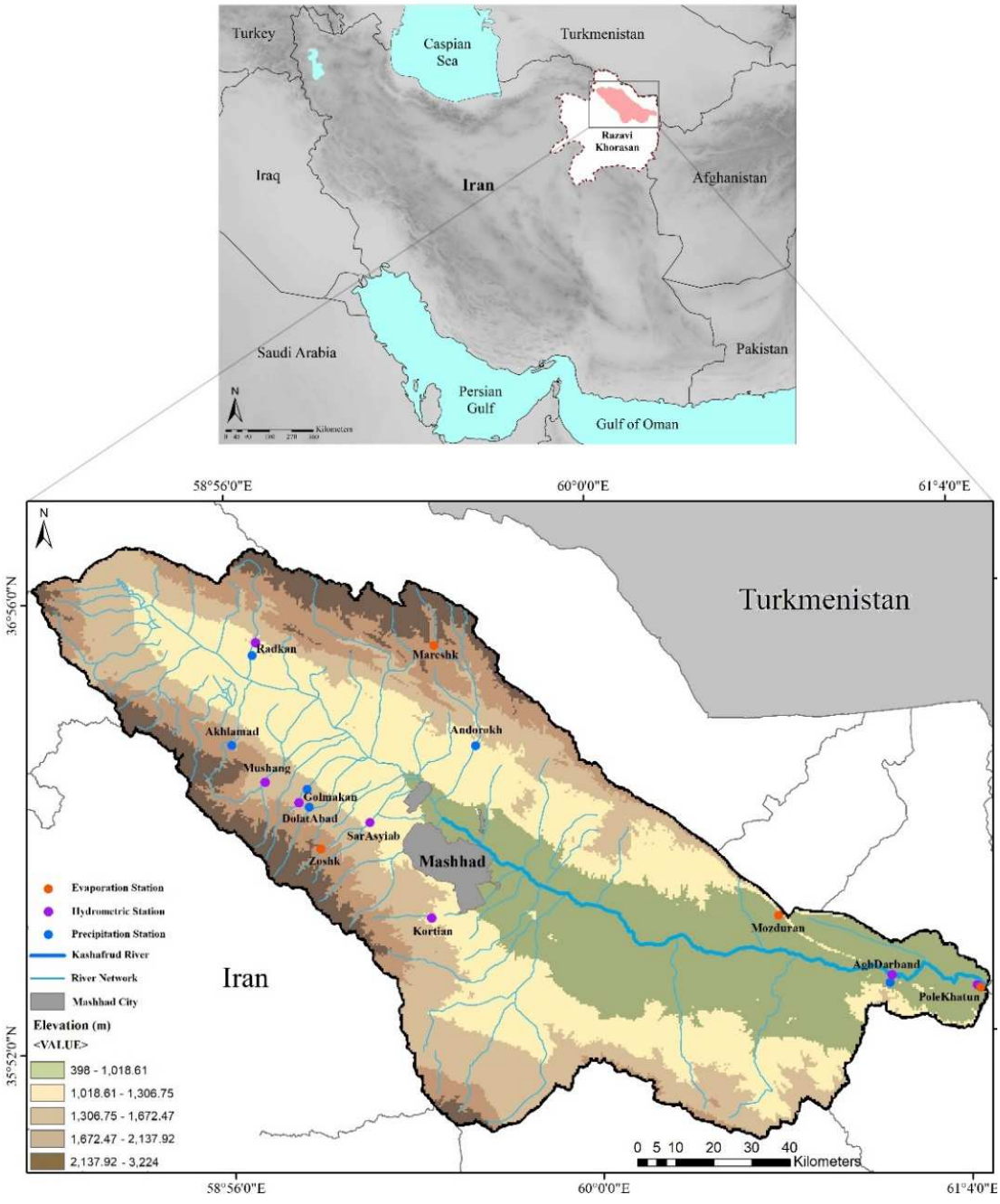


Fig. 1. Overview of the Kashafrud River Basin

Table 1. Summary of Data Used in the Study

Data Category	Parameters	Source	Temporal Coverage	Temporal Resolution	Spatial Coverage
Hydrological	Daily and monthly streamflow discharge	Razavi Khorasan Regional Water Co. (RKRWC)	1973–2023	Daily, Monthly	7 hydrometric stations across the basin (Fig. 1)
Climatic	Average monthly precipitation & temperature	Razavi Khorasan Regional Water Co. (RKRWC)	1973–2023	Monthly	Meteorological stations within the basin (Fig. 1)
Geospatial (land-use)	Land cover maps (4 classes)[1]	Landsat Satellite Imagery (1, 3, 5, 7, 9)[2]	1973, 1983, 1993, 2003, 2013, 2023	Decadal snapshots (10-year intervals)	Entire KRB

[1] Land use classes include water bodies, vegetation cover, built-up areas, and bare land.

[2] Imagery was accessed and processed using the Google Earth Engine (GEE) platform.

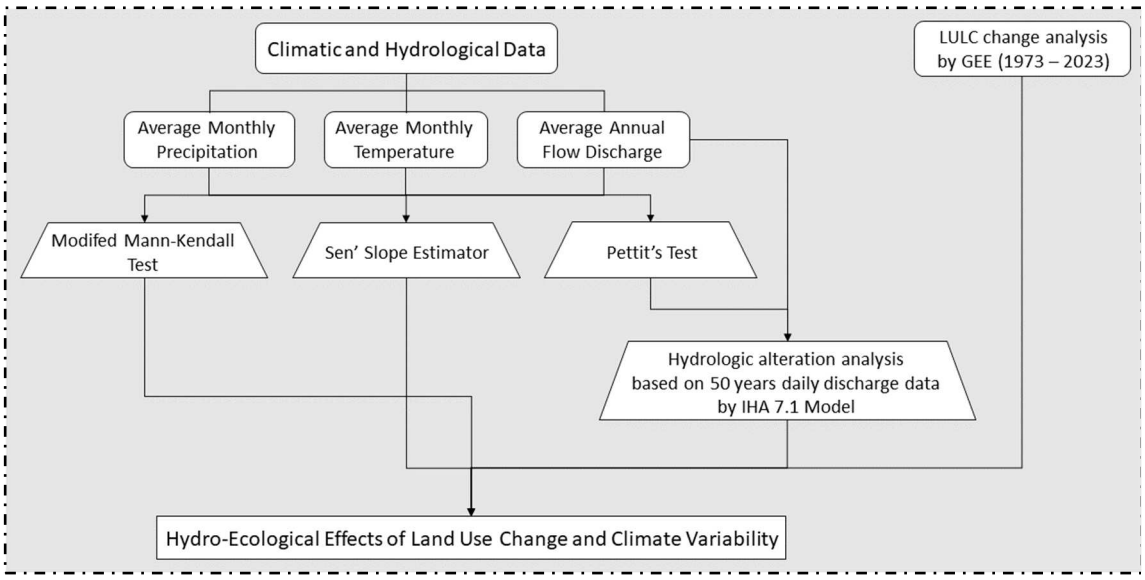


Fig 2. Flowchart of the methodology.

Trend Analysis

Trend detection tests for hydro-meteorological time series can be parametric or nonparametric (Chebana et al. 2013; Gocic & Trajkovic, 2013; Ishak et al. 2013; Xu et al. 2010). Nonparametric tests do not require the time series to be normally distributed; thus, these tests are often preferred over parametric tests in scientific communities (Abghari et al. 2013; Gocic & Trajkovic, 2013; López- Moreno et al. 2014). This study used the Mann–Kendall (MK) nonparametric test to identify statistically significant ($p<0.05$, 0.01) patterns in the hydrometeorological time series. Sen's approach (Bormann et al. 2011) was used to

determine the slope of the detected significant trends, while the Pettitt test was utilized to detect abrupt changes in the mean of the variable of interest (Villarini et al. 2009, Villarini & Smith, 2010, Liu et al. 2012; Mallakpour & Villarini, 2015).

Autocorrelation and Trend-Free Pre-Whitening (TFPW)

The presence of positive serial correlation in hydro-climatic time series can significantly inflate Type I errors, leading to the false detection of trends and abrupt change points (Bora et al. 2022). Therefore, prior to applying non-parametric tests, all datasets were examined for autocorrelation. To eliminate the effect of serial correlation while preserving the true trend structure, the Trend-Free Pre-Whitening (TFPW) approach proposed by Yue et al. (2002) was applied to the datasets.

In this procedure, the true magnitude of the trend (β) is first estimated from the original time series (Xi) using Sen's slope estimator. A detrended series (Y_i) is then generated by subtracting the linear trend from the original data:

$$Y_i = X_i - \beta \, . \, i \quad (1)$$

Next, the lag-1 autocorrelation coefficient ($r1$) of the detrended series (Yi) was calculated. This coefficient is used to remove the autoregressive component, resulting in a pre-whitened series (Y'_i).

$$Y'_i = Y_i - \mathrm{r}_1 \, . \, Y_{i-1} \quad (2)$$

Finally, the original trend is added back to the pre-whitened series to construct the final independent series (X_i), which is free of serial correlation but preserves the true trend structure.

$$X'_i = Y'_i + \beta \, . \, i \quad (3)$$

This pre-whitened independent series (X'_i) was subsequently used as the input for both the Mann–Kendall and Pettitt tests.

Mann-Kendall Test

The Mann–Kendall (Mann, 1945 & Kendall, 1946) test is a non-parametric test that has been used to assess the significance of trends in time series of selected data, such as hydro-meteorological data (Ahmad et al. 2015; Gaponov et al. 2019; Praveen et al. 2020) and has been recommended by the World Meteorological Organization for identifying hydroclimatological parameter trends. In this test, the null hypothesis assumes that there is no significant trend in the data series, and vice versa for the research hypothesis (Ahmad et al. 2015; Islam et al. 2020b). When the null hypothesis is rejected, the trend is deemed significant. The significance level at 0.05 is determined by the interval $-1.96 \leq Z \leq 1.96$, which shows no significant trends and falls under the acceptance region. When $Z < -1.96$, the trend is significantly decreasing, and when $Z > 1.96$, the trend is significantly increasing (Zhang et al. 2020). The test phases are as follows:

$$z = \frac{S - sgn(S)}{VAR(S)^{0.5}} \quad (4)$$

Where,

$$S = \sum_{i=1}^{n-1} \sum_{j=i+1}^{n} sgn(x_j - x_i) \quad (5)$$

Where, $j > i$ and $i = 1, 2..., n-1$ $j = 2, 3..., n$ and 'n' is the number of data, x_i and x_j are the data values in time series and $sgn(x_j - x_i)$ is the sign function.

$$sgn(x_j - x_i) = \begin{bmatrix} 1 & if & (x_j - x_i) > 0 \\ 0 & \text{if} & (x_j - x_i) = 0 \\ -1 & if & (x_j - x_i) < 0 \end{bmatrix} \quad (6)$$

The mean and variance of S for independent random variables with a uniform distribution and no knot (two or more data with equal numerical values following each other in an ordered series) are as follows

$$E(s)=0 \quad (7)$$

$$Var(S) = \frac{n(n-1)(2n+5)}{18} = \sigma^2$$

If there is a tied group in the data series, the variance value is calculated using the following equation, where n is the number of data points, m is the number of tied groups, and t_i is the number of ties of extent i: A tied group consists of sample data with identical values.

$$S = \frac{n(n-1)(2n+5)\sum_{i+1}^{m} t_i(i)(i-1)(2i+5)}{18} \quad (8)$$

If there are more than ten data points in a series, the standard normal test statistic Z_s is calculated as follows:

$$Zs = \begin{bmatrix} \frac{s-1}{\sigma} & if & s > 0 \\ 0 & if & \theta = 0 \\ \frac{s+1}{\sigma} & if & s < 0 \end{bmatrix} \quad (9)$$

Positive Z_s values indicate increasing trends, while negative Z_s values indicate decreasing trends. The Mann-Kendall test was calculated and tested at significant levels of 1, 5, and 10% to determine the significant hydro-climatological parameter trends. Initial trend analyses were performed using the MAKESENs software, provided by the National Iranian Meteorological Organization.

Sen's Slope Estimator

Sen's slope estimator is frequently employed in hydro-meteorological time series (Arra et al. 2025; ElNesr et al. 2010; Tabari & Marofi, 2011). Sen (1968) invented a non-parametric approach for measuring the slope of trend in a sample of N pairs of data:

$$Q_i = \frac{x_j - x_k}{j-k} \text{ for } i = 1, \dots, N, \quad (10)$$

x_j and x_k are the data values at times j and k ($j > k$), respectively. If there is only one datum in each time period, then $N=\frac{n(n-1)}{2}$; where n is the number of time periods. If there are multiple observations in one or more time periods, then $N<\frac{n(n-1)}{2}$; where n is the total number of observations.

The N values of Q_i are listed from smallest to greatest, and the median slope or Sen's slope estimator is determined as

$$Q_{med} = \begin{cases} Q\,[(N+1)/2], & \text{if } N \text{ is odd} \\ \frac{Q[N/2]+Q[(N+2)/2]}{2}, & \text{if } N \text{ is even} \end{cases} \quad (11)$$

The Q_{med} sign represents data trend reflection, and its value denotes the steepness

of the trend. To assess whether the median slope is statistically distinct from zero, we acquire the Q_{med} confidence interval with a specific probability. The confidence interval for the time slope (Frimpong et al. 2022) can be calculated as follows:

$$C_\alpha = Z_{1-\alpha/2}\sqrt{Var(S)} \quad (12)$$

where *Var(S)* is defined in Eq. (5) and $Z_{1-\alpha/2}$ is obtained from the standard normal distribution table. In this study, the confidence interval was computed at two significance levels (α = 0.01 and α = 0.05). Then, $M_1=\frac{N-C\alpha}{2}$ and $M_2=\frac{N+C\alpha}{2}$ are computed. The lower and upper limits of the confidence interval, Q_{min} and Q_{max}, are the M_1th largest and the (M_2 + 1)th largest of the *N* ordered slope estimates. If the two limits (Q_{min} and Q_{max}) are of the same sign, the slope Q_{med} is statistically distinct from zero. Sen's slope estimator for the time series were conducted using XLSTAT statistical software. XLSTAT is a data analysis and statistical application available for Microsoft Excel.

Pettitt's Test

The Pettitt test was used to detect abrupt changes in the mean of the hydroclimatic time series. This nonparametric test is based on the Mann–Whitney rank test and is suitable for identifying a single change point at an unknown time. The null hypothesis assumes that the distribution of a sequence of random variables does not change, while the alternative hypothesis assumes that the distribution function $F_1(x)$ of the random variables from X_1 to X_t is different from the distribution function $F_2(x)$ of the random variables from X_{t+1} to X_T (Mallakpour & Villarini, 2015).

$$D_{ij} = sgn(X_i - X_j) = \begin{cases} -1 & (X_i - X_j) < 0 \\ 0 & (X_i - X_j) = 0 \\ +1 & (X_i - X_j) > 0 \end{cases} \quad (13)$$

Where X_i and X_j are random variables, with X_i following X_j over time. The test statistic $U_{t,T}$ depends on D_{ij}, as follows:

$$U_{t,T} = \sum_{i=1}^{t}\sum_{j=t+1}^{T} D_{ij} \quad (14)$$

The statistic $U_{t,T}$ is the same as the Mann-Whitney statistic for determining when the two samples X_1, ..., X_t and X_{t+1} ..., X_T come from the same population. The test statistic $U_{t,T}$ is evaluated for all random variables from 1 to *T*, and the most significant change point is chosen where the value of $|U_{t,T}|$ is the greatest:

$$K_T = max_{1 \le t < T}\left|U_{t,T}\right| \quad (15)$$

A change point occurs at time *t* when the statistic K_T is substantially different from zero at the given level. The approximate significance level is provided by

$$p = 2\,.\,exp\left(\frac{-6K_T^2}{T^2+T^3}\right) \quad (16)$$

If the p-value is less than the pre-assigned significance level *α*, we reject the null hypothesis and partition the data into two sub-series (before and after the change point)

with distinct distribution functions. The Pettitt test was also implemented in XLSTAT at α =0.01 and α =0.05.

Land-Use Change Analysis

Land-use maps were generated using multi-temporal satellite imagery and remote sensing indices to assess eco-hydrological change over a 50-year period (Fig. 3). Land-use change was analyzed using Landsat imagery from six target years: 1973, 1983, 1993, 2003, 2013, and 2023 (Table 2). These dates were selected to capture major decadal transitions in the basin and to ensure temporal consistency across the study period. Owing to the lack of access to global qualified satellite data due to sanctions and political limitations, as well as the lack of a database of historical ecosystem changes in third-world countries, as well as the filtering of scientific websites for Iran, 6 specific years in the indices for the last five decades were chosen as the basis for remote sensing analysis. These years were chosen after conducting a thorough assessment of all international and national publications to identify the basin's primary difficulties that have had a direct impact on the eco-hydrological status of the KRB. The first year, 1973, was deemed the most natural state of the land cover, with no explicit human or natural calamity. Using the Shuttle Radar Topography Mission (SRTM) product, a digital elevation model (DEM) and slope layers were obtained and entered into the random forest algorithm with more than five indices, including NDVI, NDBI, NDWI, texture, and PCA (Izzati et al. 2019; Yong et al. 2021; Alam et al. 2020; Wang et al. 2021). To evaluate the classification accuracy, the available sampling points were divided into training and testing subsets, with 75% used for model training and 25% reserved for validation. Four major land-cover classes were defined: water bodies, vegetation cover, bare lands, and built-up areas. Water bodies included rivers and dam reservoirs; vegetation cover encompassed both natural vegetation and agricultural land; bare lands included exposed soil and mountainous areas; and built-up areas represented urban and rural settlements. For each target year, the area occupied by each class was calculated, and temporal changes in class extent were assessed across the five decades of observation (Chamling et al. 2020; Herrmann et al. 2020; Chen et al. 2021). The main characteristics of the satellite images used in this study are summarized in Table 2.

Table 2. Characteristics of satellite images used to monitor land use change

Year- Satellite Image	Spatial Resolution	Cloud Cover Percentage
1973-Landsat 1	30	2
1983-Landsat 3	30	2
1993-Landsat 5	30	2
2003-Landsat 5	30	2
2013-Landsat 7	30	2
2023-Landsat 9	30	2

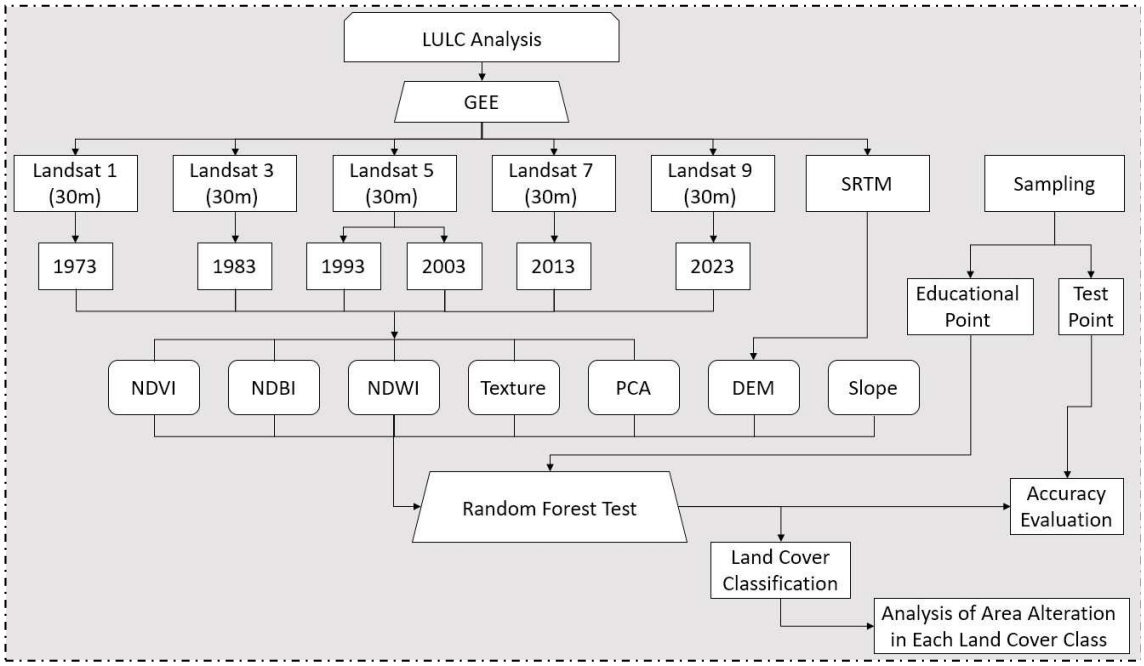


Fig 3. Land-use analysis methodology flowchart.

Accuracy Assessment

Evaluating classification accuracy is a fundamental step in remote sensing to verify the reliability and practical applicability of the generated thematic maps (Tades et al. 2020; Yonaba et al. 2021). In this study, the performance of the land use maps was quantitatively assessed using a confusion matrix. A confusion matrix was created using the validation points and classified data (Bojer et al. 2025). From these matrices, key precision metrics, namely, producer's accuracy (PA), overall accuracy (OA), and user's accuracy (UA), were derived. To further account for potential class imbalances and correct for agreement occurring by chance, the Kappa coefficient (KC) was calculated. The Kappa coefficient is particularly useful in land use classification as it provides a more robust measure of classifier consistency across all categories, preventing overrepresented classes from biasing the accuracy assessment (Li et al. 2023). The Kappa coefficient was computed using the following equation:

$$K_{hat} = \frac{N\sum_{i=1}^{n} T_{ii} - \sum_{i=1}^{n}(T_{i+}T_{+i})}{N^2 - \sum_{i=1}^{n}(T_{i+}T_{+i})} \quad (17)$$

Where N is the total number of verification points or samples for the accuracy evaluation in the confusion matrix, n is the type number of land-use data in the confusion matrix, T_{ii} is the number of land types correctly classified (the sum is the sum of the diagonals in the confusion matrix), T_{i+} represents the sum of the category in the classified data, and T_{+i} represents the sum of category i in the measured or reference data. It is used to accept the impacts of accuracy

changes, and its value shouldn't drop below 0.85 (Sajid et al. 2022).

Hydrological Alteration Analysis

The Nature Conservancy (Richter et al. 1996) proposed the indicator of hydrological alteration (IHA) as one of the most important methods for water management to identify flow characteristics that have been widely considered as primary and most important drivers of biotic and abiotic conditions in riverine ecosystems (Olden & Poff, 2003).

IHA was developed based on 33 hydrological parameters in five groups: the magnitude of monthly streamflow, the magnitude and duration of annual extreme flows, the timing of annual extreme flows, the frequency and duration of high and low pulses, and the rate and frequency of flow changes (Richter et al. 1996; Mathews & Richter, 2010, Shiau & Wu, 2008). These indicators have been widely used to evaluate eco-hydrological alterations and their implications for riverine ecosystems (Olden & Poff, 2003; Wood et al. 2000; Yang et al. 2010; Chen et al. 2013).

The range of variability approach (RVA) was used to assess hydrological changes between the pre-impact and post-impact periods (Richter, 1996; Yang et al. 2014; Shiau & Wu, 2008).

A minimum 20 years' time series of river discharge should be considered, and long-term daily data are preferred over monthly data (Mathew & Richter, 2007). The phases of the procedure are as follows:

In the pre-impact period, 33 hydrological indicators were computed.

The range of variability of each hydrological parameter will be identified. For the pre-impact IHA statistics, the range of variation between the 75th and 25th percentiles was considered the ecological target range (Zhou et al. 2020).

The 33 hydrological indicators were computed using the RVA test in the post-impact period.

The degree of hydrological modification can be calculated using the following formula:

$$D_i = \frac{(N_{0i} - N_e)}{N_e} * 100 \quad (18)$$

Where N_0 and N_e represent the observed and expected number of years, respectively, during which the post-impact values of *i*-th IHA parameter fall within the ecological target range. The thresholds for low-, medium- and high-level alteration were defined as 0 %–33 %, 33 %–66% and 66 %–100%, respectively (The Nature Conservancy, 2009).

Seven hydrometric stations were operating intermittently in the study area over the past 50 years. The final step of this study was to integrate the findings and provide a comprehensive assessment of the eco-hydrological changes in the KRB, thereby highlighting the procedures adopted for water resources management.

3. Results

Trend Test Results

Precipitation and Temperature Trend Results

The results of the trend tests for precipitation reveal significant insights into the temporal trends across different stations (Table 3, Fig. 4). DolatAbad and Andorokh Stations exhibit a statistically significant decrease in precipitation at a 99% confidence level. The negative Z-values (-3.55 and -3.42, respectively) and Sen's Slope values (-2.63 and -2.96) show a steady decrease in precipitation across the study period. The Pettitt's test finds 1997 as the change point for both stations, demonstrating that a decrease in precipitation intensified after this year. In contrast, Akhlamad, Golmakan, Radkan, and AghDarband Stations indicate no statistically significant trend (NS), indicating steady precipitation patterns over the 50 years period. P-values above 0.05 corroborate the absence of significant trends. These findings indicate that select stations within the river basin, particularly DolatAbad and Andorokh, have had significant precipitation reductions.

The temperature trend analysis indicates a statistically significant increasing trend across all stations (Table 3, Fig. 5). Mareshk, Mozduran, Pole-Khatun, and Zoshk Stations demonstrate increasing trends at 99% and 95% confidence levels. The high Z-values (ranging from 1.77 to 6.06) and positive Sen's Slope values support the rising trend in average monthly temperature. Pettitt's test identifies change points in the early 1990s (1993-1995).

Table 3. Trend Test Results for Average Monthly Precipitation and Average Monthly Temperature (1973–2023).

Trend Test Results for Precipitation												
No.	Station Name	Mann-Kendall Test			Sen's Slope Test					Pettitt's Test		
		Trend Alteration	Conf. Level	Z test	Sen's Slope	Confidence Level				Change Point	Conf. Level	P Value
						Qmax95	Qmin95	Qmax99	Qmin99			
1	Akhlamad	-	NS	0.07	0.02	1.31	-1.22	1.75	-1.66	-	NS	0.738
2	DolatAbad	Decreasing	99%	-3.55	-2.63	-1.12	-4.30	-0.58	-4.95	1997	99%	0.0002
3	Golmakan	-	NS	0.98	0.77	2.38	-0.94	2.98	-1.50	-	NS	0.80
4	Radkan	-	NS	-1.13	-0.68	0.62	-2.00	0.97	-2.48	-	NS	0.23
5	Andorokh	Decreasing	99%	-3.42	-2.96	-1.03	-5.00	-0.49	-5.50	1997	99%	0.0006
6	AghDarband	-	NS	0.14	0.10	1.94	-1.83	2.73	-2.59	-	NS	0.603
Trend Test Results for Temperature												
No.	Station Name	Mann-Kendall Test			Sen's Slope Test					Pettitt's Test		
		Trend Alteration	Conf. Level	Z test	Sen's Slope	Confidence Level				Change Point	Conf. Level	P Value
						Qmax95	Qmin95	Qmax99	Qmin99			
1	Mareshk	Increasing	99%	4.73	0.10	0.12	0.09	0.12	0.08	1995	99%	<0.0001
2	Mozduran	Increasing	99%	6.06	0.05	0.07	0.04	0.07	0.03	1995	99%	<0.0001
3	Pole-Khatun	Increasing	99%	5.13	0.04	0.05	0.02	0.06	0.01	1993	99%	<0.0001
4	Zoshk	Increasing	90%	1.77	0.01	0.02	0.002	0.03	-0.002	1993	95%	0.027

Our analysis highlights a major warming trend in the KRB. The trend analysis shows a twofold pattern: a considerable decrease in precipitation at some stations and a general increase in temperature at all stations. The identification of change points in the 1990s suggests a shift in the hydro-climatic regime of the KRB.

Flow Discharge Trend Results

The analysis of the average annual flow discharge over the period 1973–2023 reveals a significant decreasing trend at most stations (Table 4, Fig. 6). Radkan, Golmakan, Kortian, Mushang, Pole-Khatun, and SarAsiab Stations exhibited statistically significant decreasing trends with confidence levels ranging from 90% to 99%. The negative Z-values and negative Sen's Slope values indicate a constant reduction in flow discharge.

Pettitt's test identifies change points in 1998 for Radkan and Kortian stations and in 1983 for Pole-Khatun station, representing important periods when the reduction in flow increased. In contrast, AghDarband Station show no statistically significant trend.

The analysis of the time series at the downstream stations (AghDarband and Pole-Khatun) provides a clear framework for understanding these hydrological variations. At Pole-Khatun, the significant decreasing trend in flow discharge strongly aligns with

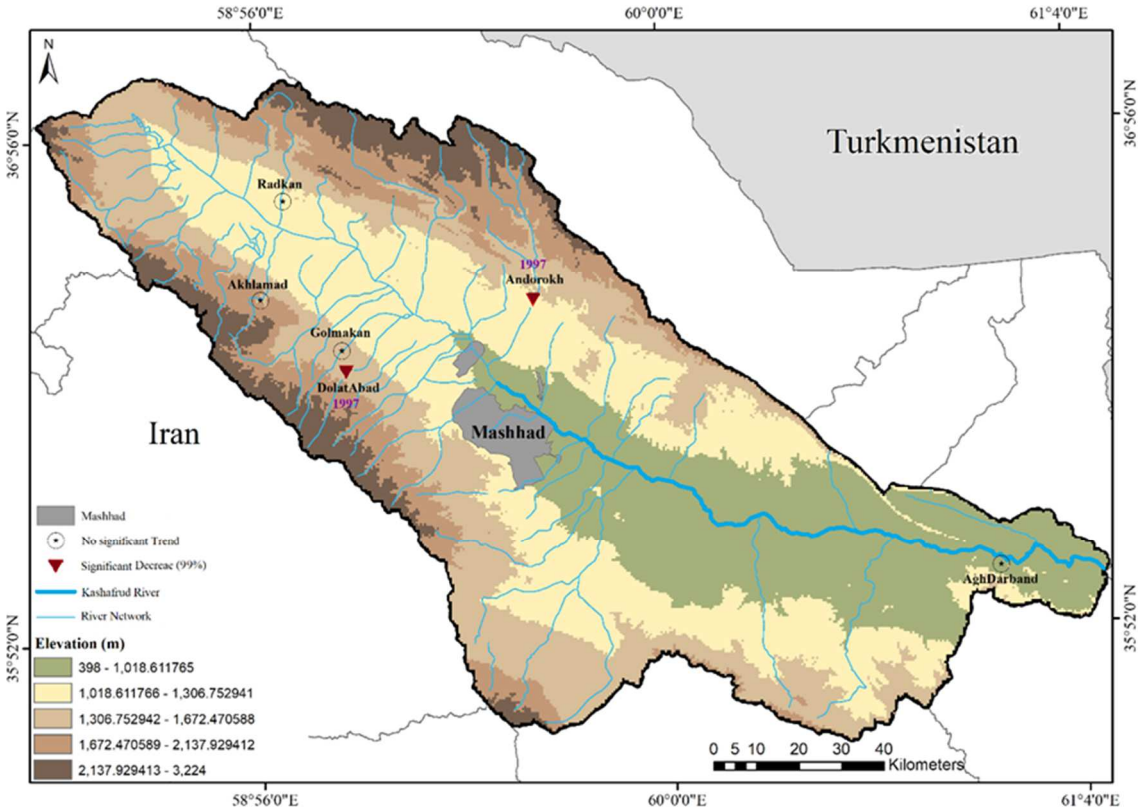


Fig 4. Results of Trend Tests for Precipitation of the Kashafrud River Basin and Their Abrupt Change Years (1973-2023).

the statistically significant increasing temperatures observed at this station (at 95% and 99% confidence levels). In contrast, the AghDarband station exhibits stable flow patterns, which correspond directly to its steady precipitation records (showing no statistically significant decreasing trend). Overall, the trend analysis demonstrates a twofold pattern across the basin: an overarching rise in temperature across all stations, combined with localized drops in precipitation and streamflow that severely impact downstream availability at stations like Pole-Khatun.

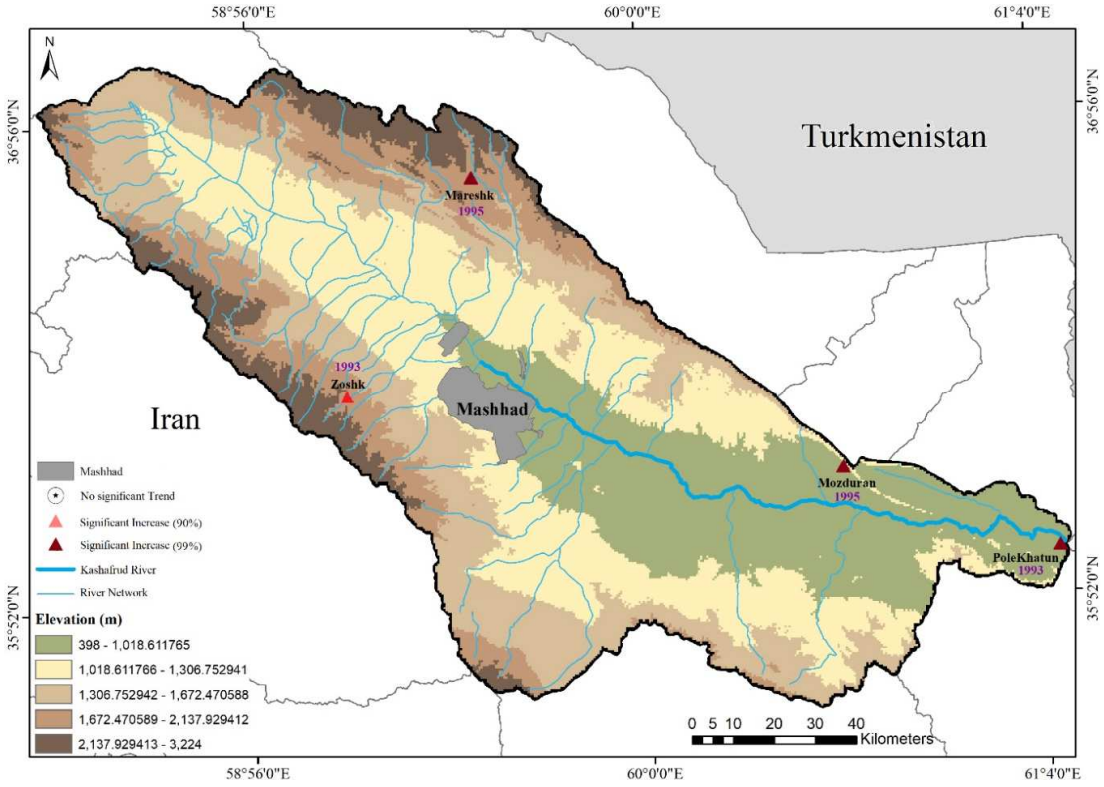


Fig 5. Results of Trend Tests for Temperature of the Kashafrud River Basin and Their Abrupt Change Years (1973-2023).

Table 4. Trend Test Results for Average Annual Flow (1973–2023)

Trend Test Results for Flow Discharge												
No.	Station Name	Mann-Kendall Test			Sen's Slope Test					Pettitt's Test		
		Trend Alteration	Conf. Level	Z test	Sen's Slope	Confidence Level				Change Point	Conf. Level	P Value
						Qmax95	Qmin95	Qmax99	Qmin99			
1	AghDarband	-	NS	-1.49	-0.012	0.006	-0.035	0.015	-0.044	-	NS	0.651
2	Radkan	Decreasing	90%	-1.86	-0.005	-0.001	-0.009	0.000	-0.011	1998	99%	0.0002
3	Golmakan	Decreasing	95%	-2.20	-0.003	0.000	-0.006	0.001	-0.007	-	NS	0.139
4	Kortian	Decreasing	99%	-2.94	-0.009	-0.003	-0.016	-0.001	-0.018	1998	95%	0.011
5	Mushang	Decreasing	95%	-2.25	-0.015	0.002	-0.034	0.009	-0.039	-	NS	0.214
6	Pole-Khatun	Decreasing	95%	-2.02	-0.030	-0.005	-0.057	0.002	-0.067	1983	95%	0.031
7	SarAsiab	Decreasing	90%	-1.91	-0.007	0.001	-0.013	0.004	-0.015	-	NS	0.657

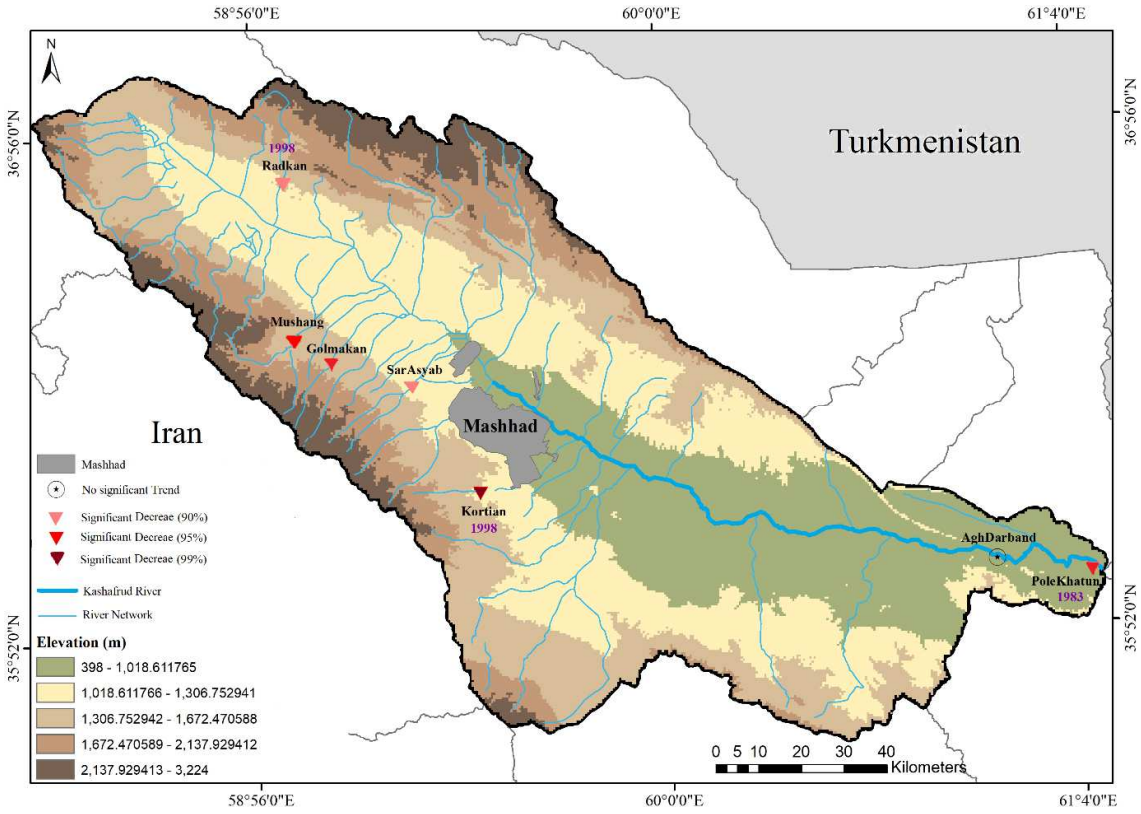


Fig 6. Results of Trend Tests for Average Annual Flow at Hydrometric Stations of the Kashafrud River Basin and Their Abrupt Change Years (1973–2023).

Land-Use Change Results

The results of monitoring land-use changes in the KRB over five decades (1973–2023) reveal significant transformations driven by agricultural expansion, urbanization, and land degradation (Fig. 7). The consistent increase in agricultural land from 13.44% in 1973 to 18.23% in 2023.

In contrast, water bodies have experienced minimal fluctuations, with a slight decline from 0.08% in 1973 to 0.05% in 2023, indicating relative stability in surface water resources.

Rangeland has declined dramatically, falling from 58.20% in 1973 to 36.98% in 2023. In contrast, bare land has increased dramatically, going from 27.01% to 42.49% during the same period. Furthermore, built-up areas have steadily increased from 1.27% in 1973 to 2.24% in 2023.

Land-Use Classification Accuracy

The accuracy assessment metrics for the classified land-use maps across the six study periods are summarized in Table 5. The overall classification accuracy ranged from a minimum of 84.15% in 1973 to a maximum of 92.31% in 1993, consistently exceeding the standard acceptable threshold of 85% for most years (with 1973 being marginally below at 84.15%). The Kappa coefficient statistics varied between 78.42% (1973) and

87.59% (1993), representing substantial to almost perfect agreement between the classification results and reference data.

Class-specific accuracies revealed high reliability, particularly for the water body class, which consistently achieved 100% user accuracy (UA) and producer accuracy (PA) across all years owing to its distinct spectral signature. The bare land and rangeland classes also exhibited high and stable accuracies, with UA and PA values generally exceeding 80%–90%. For the agricultural area class, PA values reached 100% in 2013 and 2023, although UA dropped to 62.50% and 57.89% in those respective years, reflecting some spectral mixing between active agricultural plots and surrounding natural vegetation or rangelands during those periods. Similarly, the built-up area class exhibited strong performance, with UA reaching 100% in 2013 and PA peaking at 100% in 1993. Overall, these validation metrics confirm that the generated land-use datasets are highly reliable for subsequent change detection and hydrological impact analysis.

Hydrological alteration and IHA results

To investigate the impact of climate variability and land-use alterations on the hydrology of the KRB, the Indicators of Hydrologic Alteration (IHA) framework was applied to seven hydrometric stations. Based on the results of the Mann–Kendall trend test, Sen's slope estimator, and Pettitt's test for annual streamflow (discussed in Section 3.1.2), stations exhibiting significant trends and change points were prioritized. These stations include: 1. Radkan (decreasing trend, change point: 1998), 2. Kortian (decreasing trend, change point: 1998), and 3. Pole-Khatun (decreasing trend, change point: 1983). The Pole-Khatun station, located at the basin outlet, is especially crucial because its IHA analysis reflects the cumulative basin-wide effects of upstream land-use transformations and climatic shifts.

Table 5. Accuracy assessment metrics of the land-use classification for the study period (1973–2023)

Land-Use classes	1973		1983		1993		2003		2013		2023	
	UA (%)	PA (%)	UA (%)	PA (%)	UA (%)	PA (%)	UA (%)	PA (%)	UA (%)	PA (%)	UA (%)	PA (%)
Agricultural Area	76.40%	81.50%	81.20%	78.90%	88.89%	84.21%	86.50%	82.30%	62.50%	100.00%	57.89%	100.00%
Bare land	88.20%	83.60%	90.50%	85.10%	95.00%	86.36%	92.10%	88.50%	85.37%	87.50%	94.87%	90.24%
Built Area	82.10%	85.00%	78.50%	88.20%	85.71%	100.00%	89.00%	94.10%	100.00%	90.91%	80.00%	80.00%
Water Body	100.00%	100.00%	100.00%	100.00%	100.00%	100.00%	100.00%	100.00%	100.00%	100.00%	100.00%	100.00%
Rangeland	85.50%	82.30%	88.00%	87.50%	92.54%	95.38%	91.20%	89.40%	92.68%	80.85%	100.00%	85.71%
Overall accuracy	84.15%		85.60%		92.31%		89.45%		87.29%		88.89%	
Overall, Kappa Statistics	78.42%		80.15%		87.59%		85.20%		82.28%		83.13%	

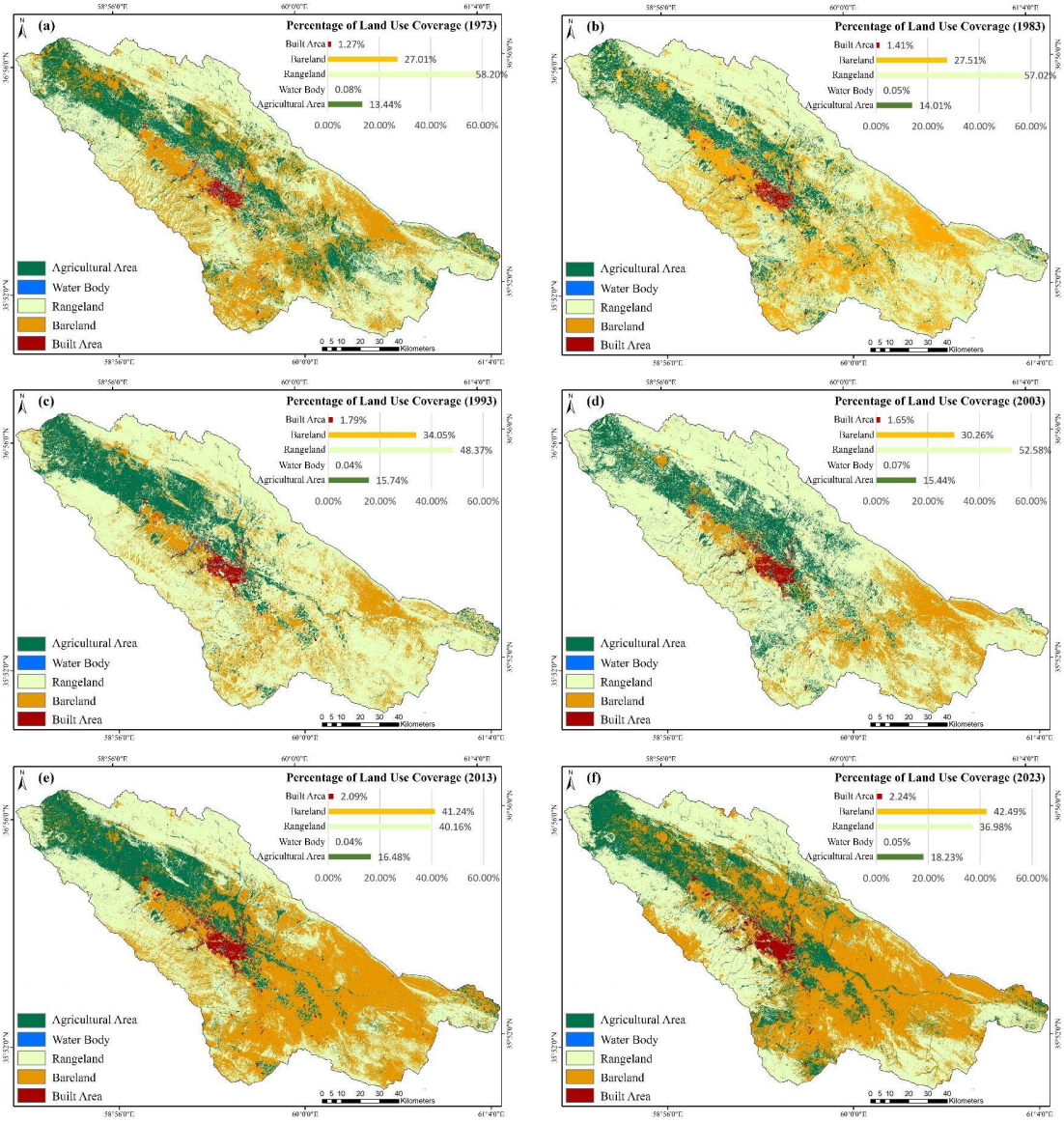


Fig 7. Land use changes in the Kashafrud River Basin (1973–2023).

The IHA analysis reveals significant hydrological alterations directly linked to the previously identified climatic and land use changes. The magnitude of monthly flows has decreased significantly, especially in winter and spring, with the Radkan station showing substantial losses in February (-76%), April (-76%), and November (-87%). At the downstream Pole-Khatun station, an extreme flow loss of -93.16% was observed in July. These severe reductions are not isolated; they correspond directly to the significant temperature increases and drastic expansion of agricultural lands (from 13.44% to 18.23%) reported in previous sections.

Extreme flow conditions further illustrate this disruption. Minimum flows show severe declines, notably at Radkan, where 1-day and 3-day minimum flows decreased by 100%. This total loss of base flow is a direct consequence of prolonged droughts and diminished groundwater recharge caused by widespread vegetation removal. Conversely, maximum flows show a mixed pattern at Radkan, decreasing at longer durations (7- to 30-day: -21.74% to -47.83%) while increasing at shorter durations (1- to 3-day: +44% to +56.52%); at Pole-Khatun, however, maximum flows declined consistently across all durations, reaching -79.47% at the 30-day scale. The timing and frequency of hydrological pulses have also shifted dramatically. Minimum flows occurred earlier (by 14–17%), and high-pulse frequencies increased at Radkan (+17.39%) and Kortian (+9.56%).

The output graphs of long-term monthly flow discharge alteration for the three selected stations are presented in Fig. 8, and a comparison between the natural flow regime before and after the change points.

Table 6. Results of 33 indicators of hydrologic alteration at three hydrometric stations

Station Name	Index Parameters	Radkan	Kortian	Pole-Khatun
Index Group		Hydrologic Alteration Result		
Group 1 Magnitude of monthly water conditions	1- Mean flow in January	-47.83%-M	40.96%-M	40.64%-M
	2- Mean flow in February	-76-H	-79.71%-H	-65.79%-M
	3- Mean flow in March	-60.87%-M	-39.13%-M	-72.63%-H
	4- Mean flow in April	-76-H	-87.83%-H	-45.26%-M
	5- Mean flow in May	-64.78%-M	-22.53%-L	-58.95%-M
	6- Mean flow in June	-17.83%-L	-14.78%-L	-71.49%-H
	7- Mean flow in July	-60.87%-M	-26.96%-L	-93.16%-H
	8- Mean flow in August	-60.87%-M	-14.78%-L	-17.89%-L
	9- Mean flow in September	-47.83%-M	-14.78%-L	-45.26%-M
	10- Mean flow in October	-74-H	34.55%-M	29.24%-L
	11- Mean flow in November	-87-H	16.67%-L	19.74%-L
	12- Mean flow in December	-87-H	7.69%-L	-0.79%-L
Group 2 Magnitude and duration of annual extreme water conditions	13- 1 d minimum	-100-H	3.70%-L	-7.90%-L
	14- 3 d minimum	-100-H	3.70%-L	-7.90%-L
	15- 7 d minimum	-73-H	3.70%-L	-7.90%-L
	16- 30 d minimum	-87-H	7.69%-L	-11.62%-L
	17- 90 d minimum	-74-H	28.15%-L	36.84%-M
	18- 1 d maximum	44-M	46.09%-M	-38.42%-M
	19- 3 d maximum	56.52%-M	9.57%-L	-52.11%-M
	20- 7 d maximum	-21.74%-L	21.74%-L	-58.95%-M
	21- 30 d maximum	-47.83%-M	-2.61%-L	-79.47%-H
	22- 90 d maximum	-34.78%-M	-14.78%-L	-72.63%-H
	23- Base flow index	-45.82%-M	-75.65%-H	-79.47%-H
	24- Zero-flow day	-60.87%-M	3.70%-L	-7.90%-L

Continue Table 6.

Station Name	Index Parameters	Radkan	Kortian	Pole-Khatun
Index Group		**Hydrologic Alteration Result**		
Group 3 Timing of annual extreme water conditions	25- Date of minimum	17.39%-L	16.67%-L	14.04%-L
	26- Date of maximum	-21.74%-L	-33.60%-M	23.16%-L
Group 4 Frequency and duration of high and low pulse	27- Low-pulse count	-11.96%-L	-18.84%-L	-65.79%-M
	28- Low-pulse duration	-41.30%-M	-39.13%-M	-31.58%-L
	29- High-pulse count	17.39%-L	9.56%-L	-31.58%-L
	30- High-pulse duration	-11.96%-L	-2.61%-L	-58.95%-M
Group 5 Rate and frequency of water condition change	31- Rise rate	-79-H	9.57%-L	-31.58%-L
	32- Fall rate	-79-H	-11.46%-L	-58.95%-M
	33- Number of reversals	-53.04%-M	-22.53%-L	-42.98%-M

H: High, M: Moderate, L: Low

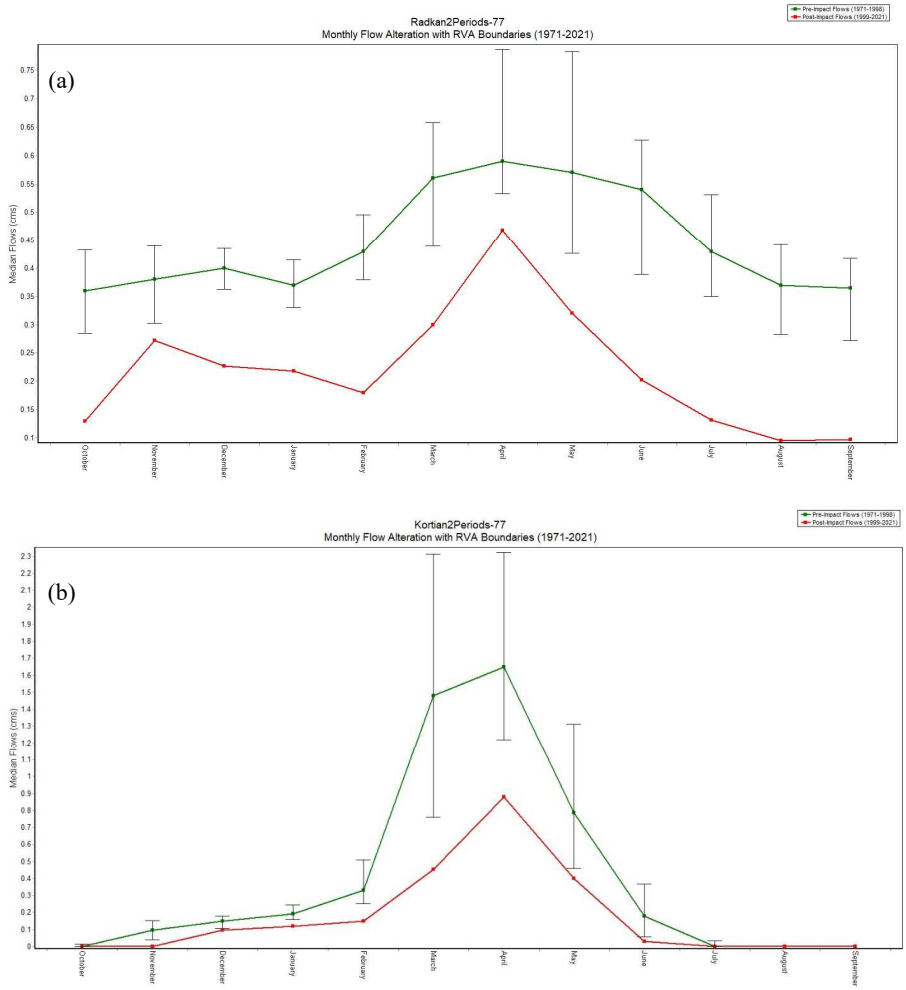
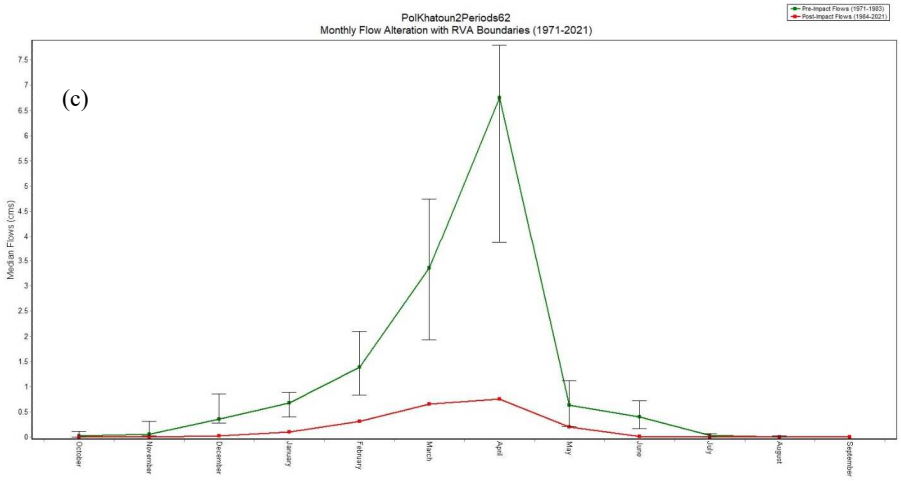


Fig 8. Monthly streamflow discharge over the last 50 years with RVA boundaries for (a). Radkan Station, (b). Kortian Station, and (c). Pole -Khatun Station.



Continue Fig 8.

4. Discussion

Interplay of climate variability, Land-use dynamics, and IHA-based streamflow alterations

The integration of meteorological trends, land-use dynamics, and indicators of hydrologic alteration (IHA) from 1973 to 2023 indicates substantial changes in the KRB's hydrological regime. Rather than acting in isolation, the observed meteorological shifts and land-use transformations appear to be jointly associated with changes in the magnitude, frequency, and timing of streamflow. The statistically significant drop in precipitation at key stations such as DolatAbad and Andorokh, punctuated by a regime shift around 1997, coincided with a persistent increase in temperature beginning in the early 1990s. This warming pattern, consistent with global trends and supported by broader national studies (Kousari et al. 2013; Saboohi et al. 2012; Tabari & Talaee, 2011; Zarenistanak et al. 2014), may have increased atmospheric evaporative demand and contributed to changes in the basin's water balance.

When analyzing these climatic shifts through the lens of the IHA model, the mechanistic linkages become clear. The severe reduction in monthly flow magnitudes (IHA Group 1) and the dramatic decline in extreme minimum flows (IHA Group 2), including the near-total loss of base flow during dry seasons, are not merely symptoms of reduced rainfall. As similarly documented in other Iranian basins, including the Lake Urmia basin in northwest Iran (Nazeri Tahroudi et al. 2019) and the Shahpour River basin in south Iran (Fooladi et al. 2021), the combination of declining precipitation and rising temperatures has severely diminished both surface runoff generation and groundwater recharge. In the KRB, this climatic stress is further compounded by

localized evapotranspiration increases driven by rising temperatures (Baygi et al. 2023), systematically draining the basin's natural water storage and depressing seasonal flow volumes. Furthermore, the remote sensing evidence of land-use changes, characterized by the significant expansion of built-up areas and agricultural lands at the expense of natural vegetation, explains the specific alterations in IHA pulse dynamics and flow rates (IHA Groups 4 and 5). The transition from natural vegetative cover to impervious urban surfaces physically alters the watershed's response by reducing soil infiltration capacity and accelerating surface runoff. This mechanism is directly responsible for the increased frequency of high-flow pulses and the increasingly "flashy" nature of the hydrograph observed in the IHA results. The dramatic conversion of natural rangelands (from 58.20% to 36.98%) into bare lands (increasing to 42.49%) and agricultural fields fundamentally alters the basin's water balance by removing natural vegetation cover. This loss of vegetation significantly decreases canopy interception and reduces soil organic matter, which in turn diminishes soil permeability and infiltration rates. Consequently, natural groundwater recharge processes are impaired, leading to a severe reduction in the sustained base flow that feeds the Kashafrud River. Furthermore, the continuous expansion of agricultural lands (from 13.44% to 18.23%) directly amplifies the basin's actual evapotranspiration (ET). Intensive agricultural practices and the corresponding increase in crop water demand, especially when combined with the rising regional temperatures identified in the climatic analysis, create a synergistic effect. This heightened ET extracts massive volumes of water from both soil moisture and shallow aquifers before it can reach the river network. Additionally, the expansion of built-up areas (from 1.27% to 2.24%) increases impervious surface coverage, further restricting local infiltration and altering natural flow dynamics. Ultimately, the compounded effects of these mechanisms, decreased soil permeability and water retention capacity due to land degradation, alongside significantly enhanced evapotranspiration from expanded agriculture and rising temperatures, provide a clear physical explanation for the substantial declining trends in river flow, severely impacting downstream water availability. Gholizadeh et al. (2021) identified analogous processes in the Mashhad basin, noting that urbanization severely curtails natural groundwater recharge. Simultaneously, unsupervised agricultural development has introduced profound anthropogenic forcing. The expansion of cultivated areas has increased water demand well beyond the natural carrying capacity of the basin. This has driven intense, often unrecorded, surface water diversions and groundwater pumping, further flattening the hydrograph and homogenizing the rate and frequency of

water condition changes (IHA Group 5). Consequently, the integration of these findings moves beyond recognizing simple trends; it demonstrates a compounding feedback loop where climate warming (increasing demand and evaporation) and land-use degradation (decreasing infiltration and increasing withdrawals) converge to dismantle the natural flow regime. Understanding these interrelated dynamics is paramount, as they underscore the critical need for integrated watershed management strategies that holistically address land-use regulation and climate adaptation to restore ecological flow requirements.

Hydrological alteration and potential ecological implications

Hydrological regimes dictate the physical framework within which riverine ecosystems evolve and function. In the KRB, the integration of Indicator of Hydrologic Alteration (IHA) outputs reveals that climatic variability and shifting land use have pushed the river system beyond its historical ecological baseline. The critical change points identified in the streamflow time series (e.g., during the 1980s and late 1990s across various stations) do not merely represent statistical shifts; rather, they mark severe ecological tipping points. Such structural alterations in the natural flow regime decouple the temporal synchronization between hydrological events and the life-cycle requirements of native aquatic biota, severely threatening the ecological integrity and resilience of riverine habitats (Wang et al. 2017; Yang et al. 2017). It is important to clarify that the ecological implications discussed in this study are inferred from alterations in the hydrological regime and rely on established hydro-ecological principles. The study does not provide direct empirical biological data (e.g., biodiversity or habitat surveys); rather, it focuses on identifying hydrological stressors that may compromise the ecological integrity of the riverine system.

Ecologically, the loss of seasonal flow disrupts aquatic habitats, reduces spawning grounds for native fish, and concentrates pollutants during low-flow months, while the absence of natural high-flow events impairs channel flushing, leading to sediment accumulation, loss of deep-water refuges, and degradation of riparian geomorphology, posing a critical threat to aquatic biodiversity. Extended periods of extreme minimum flows and the potential desiccation of the river channel during dry seasons lead to severe habitat fragmentation, thermal stress, and reduction in dissolved oxygen levels. Aquatic species that rely on stable, continuous base flows for survival and reproduction are highly vulnerable to these conditions. This mechanism of habitat degradation directly mirrors the findings of Morid et al. (2016) in the Kordan River, where the depletion of base flows systematically dismantled critical fish habitats and threatened local aquatic populations.

Furthermore, the altered timing of high-flow episodes and the intensification of runoff pulses, largely driven by urban expansion and increased impervious surfaces, introduce destructive physical forces into the channel. Rapid, unbuffered urban runoff increases stream power during storm events, leading to severe riverbank erosion, scouring of the benthic substrate, and elevated suspended sediment loads. These processes destroy spawning grounds by burying gravel beds in sediment and disrupt the biochemical balance of the water column. Similar degradation has been well documented in the Shahrchai River by Mostafazadeh et al. (2024), who demonstrated that accelerated anthropogenic land use fundamentally destabilized hydrological indices and exacerbated sediment-driven ecological degradation.

Beyond the main river channel, the ecological consequences extend to the riparian zone interactions. The substantial expansion of agricultural activities and associated groundwater overexploitation has drastically curtailed natural groundwater recharge. This drawdown of the water table disconnects the river from its floodplain, inflicting severe moisture stress on riparian vegetation that depends on shallow groundwater. This cascading effect is consistent with the extensive evaluation by Parizi et al. (2020) across Iran, which highlighted how declining groundwater recharge rates systematically degrade vegetative cover and reduce overall basin biodiversity.

To mitigate these compounding ecological crises, transitioning toward adaptive and integrated water resource management is imperative. Restoring elements of the natural flow regime, often referred to as environmental flows through regulated reservoir releases, is critical to re-establishing essential base flows and high-flow ecological cues. Concurrently, implementing nature-based solutions, such as maintaining robust riparian buffer zones to filter sediments and adopting sustainable agricultural practices to minimize unseasonal runoff, can significantly enhance habitat connectivity and resilience (Gatgash & Sadeghi, 2024; Guo et al. 2024). Ultimately, mainstreaming coupled eco-hydrological modeling into regional planning is essential to balance human water demands with the critical imperative of biodiversity protection in the KRB.

5. Advantages and limitations

This study proposes an integrated research methodology that combines the Indicator of Hydrologic Alteration (IHA) method, remote sensing, and robust statistical tests to assess streamflow dynamics and their ecological implications in the KRB. A fundamental advantage of this approach is its ability to identify significant transition points and temporal shifts in the flow regime, which is crucial for directing future streamflow

projections and ecological conservation strategies (Liu et al. 2024). By incorporating the IHA technique, this study provides a comprehensive assessment of the potential ecological implications of streamflow alterations, including possible habitat degradation and changes in environmental flow conditions, which are often overlooked in conventional hydrological research. Furthermore, combining multi-period land-use imagery via Google Earth Engine significantly improves the spatial accuracy of identifying anthropogenic footprint expansion and its concurrent effects on hydrological dynamics (Torabi Haghighi et al. 2020). The application of robust statistical approaches, including the Mann-Kendall test, Sen's slope estimator, and Pettitt's test, equips the study with dependable tools for detecting monotonic trends and abrupt change points in long-term climatic and hydrological time series (Malede et al. 2022). Despite these strengths, the current methodology exhibits certain limitations that should be addressed in future research. Primarily, while the study establishes strong associative evidence between environmental drivers and hydrological changes, it does not employ explicit statistical or physical attribution methods (such as the Budyko framework, hydrological sensitivity analysis, process-based- watershed modeling (e.g., SWAT scenario simulations), or statistical variance decomposition- techniques) to quantitatively separate the fractional contributions of climate variability versus land-use changes. Consequently, the findings provide a qualitative understanding of overlapping drivers rather than a quantified variance decomposition. Another notable limitation is the reliance on historical data quality and availability, which might impair the accuracy of trend detection, particularly in stations with incomplete discharge and climate records (Liu et al. 2024). This study, like all long-term hydro-climatic analyses, is subject to several sources of uncertainty. These include potential measurement inconsistencies in station records, uncertainty introduced by regression-based infilling of missing data, and the inherent variability of hydro-climatic systems that affect trend detection even when the Mann-Kendall test is used to mitigate serial correlation bias. These uncertainties should be considered when interpreting the magnitude of detected trends. Furthermore, the IHA approach focuses predominantly on surface water dynamics, meaning that complex groundwater-surface water interactions and aquifer depletion are not fully integrated into the ecological assessment. Finally, inherent uncertainties in global climate models and future forecasts complicate the projection of long-term hydrological responses, potentially affecting the reliability of proposed adaptation measures (Nazeri Tahroudi et al. 2018). Addressing these gaps through advanced quantitative attribution models and coupled eco-hydrological frameworks will further solidify the understanding of watershed dynamics.

6. Conclusion

This study applied an integrated methodology combining robust nonparametric hydro-climatic analysis, multi-temporal satellite-based land-use mapping, and eco-hydrological alteration metrics (IHA/RVA) to evaluate long-term changes in the KRB from 1973 to 2023. The data show a substantial decrease in precipitation and a consistent increase in temperature, which were associated with notable hydrological changes. The use of the Indicators of Hydrologic Alteration (IHA) framework indicated significant variations in flow regimes, such as changes in low-flow situations, peak discharge time, and total flow variability. These shifts suggest that climate variability and anthropogenic land-use changes may have contributed to changes in the basin's natural hydrological equilibrium. Our findings indicate that the DolatAbad and Andorokh stations experienced the most pronounced precipitation declines, with statistically significant shift points identified in the late 1990s. Concurrently, all monitored stations exhibited a consistent warming trend, aligning with broader regional and global climatic patterns. These climatic shifts may have increased evapotranspiration and contributed to changes in the frequency and magnitude of streamflow. Furthermore, land-use analysis revealed that built-up areas and agricultural lands expanded at the expense of natural vegetation, a pattern that may be associated with increased hydrological stress, higher surface runoff potential, and reduced groundwater recharge potential. Hydrological alterations identified by IHA analysis show an increase in flow irregularity, with lower base flows and more erratic peak flows. These changes may pose risks to the ecological stability of the river system, with potential implications for aquatic habitats, sediment transport, and water supply for downstream consumers. The fall in low flows, in particular, poses threats to water security and ecosystem health, prompting immediate action through adaptive water resource management. Despite the study's robustness, certain limitations remain, including the lack of high-resolution climate projections and potential uncertainties in land-use classification. Future studies should use improved hydrological models and scenario-based climate forecasts to improve forecasting accuracy. Furthermore, sustainable land management strategies, better irrigation techniques, and integrated watershed management approaches are critical for mitigating the negative consequences of climate variability and land-use alterations.

In conclusion, this study emphasizes the critical necessity for comprehensive water resource planning in the KRB. Given the continued climatic and anthropogenic pressures, proactive interventions, such as conservation farming and enhanced water governance, are essential for long-term hydrological sustainability. Policymakers can improve the resilience of the basin's water resources by combining climate adaptation methods with sustainable land-use practices, protecting ecological integrity, and supporting socio-economic development in the region.

References

Abghari, H., Tabari, H., & Talaee, P. H. (2013). River flow trends in the west of Iran during the past 40 years: impact of precipitation variability. *Global and Planetary Change*, *101*, 52-60.

Ahmad, I., Tang, D., Wang, T., Wang, M., & Wagan, B. (2015). Precipitation Trends over Time Using Mann-Kendall and Spearman's rho Tests in Swat River Basin, Pakistan. *Advances in Meteorology*, *2015*(1), 431860.

Alam, A., Bhat, M.S. & Maheen, M. 2020.Using Landsat satellite data for assessing the land use and land cover change in Kashmir valley. GeoJournal 85, 1529–1543. https://doi.org/10.1007/s10708-019-10037-x.

Arra, A. A., Keskin, M. Z., & Şişman, E. (2025). Trend analysis of hydro-meteorological variables using Mann-Kendall and Sen's Slope with Standardization (SSS): Case study of the Kızılırmak catchment, Türkiye. Physics and Chemistry of the Earth, Parts A/B/C, 104115.

Baygi, R. K., Ghezelsofloo, A. A., Eftekhari, M., & Rastgoo, M. (2023). Journal of Drought and Climate change Research (JDCR). *Journal of Drought and Climate change Research (JDCR)*, *1*(2), 27-40.

Bekele, D., Alamirew, T., Kebede, A., Zeleke, G., & M. Melesse, A. (2019). Modeling climate change impact on the Hydrology of Keleta watershed in the Awash River basin, Ethiopia. *Environmental Modeling & Assessment*, *24*, 95-107.

Bojer, A. K., Abshare, M. W., Mesfin, F., & Al-Quraishi, A. M. F. (2025). Assessing climate and land use impacts on surface water yield using remote sensing and machine learning. Scientific Reports, 15(1), 18477.

Bora, S. L., Bhuyan, K., Hazarika, P. J., Gogoi, J., & Goswami, K. (2022). Analysis of rainfall trend using non-parametric methods and innovative trend analysis during 1901–2020 in seven states of North East India. *Current Science*, *122*(7), 801-811.

Bormann, H., Pinter, N., & Elfert, S. (2011). Hydrological signatures of flood trends on German rivers: Flood frequencies, flood heights and specific stages. *Journal of Hydrology*, *404*(1-2), 50-66.

Chamling, M., Bera, B. Spatio-temporal Patterns of Land Use/Land Cover Change in the Bhutan–Bengal Foothill Region Between 1987 and 2019: Study towards Geospatial Applications and Policy Making. Earth Syst Environ 4, 117–130 .2020. https://doi.org/10.1007/s41748-020-00150

Chebana, F., Ouarda, T. B., & Duong, T. C. (2013). Testing for multivariate trends in hydrologic frequency analysis. *Journal of hydrology*, *486*, 519-530.

Chen X, Yang T, Wang XY .2013. Uncertainty intercomparison of different hydrological models in simulating extreme flows. Journal of Water Resource Management 27:1393.

Chen, W., Zeng, J., & Li, N. (2021). Change in land-use structure due to urbanisation in China. *Journal of Cleaner Production*, *321*, 128986.

De Girolamo, A. M., Barca, E., Leone, M., & Porto, A. L. (2022). Impact of long-term climate change on flow regime in a Mediterranean basin. Journal of Hydrology: Regional Studies, 41, 101061.

Dibaba, W. T., Demissie, T. A., & Miegel, K. (2020). Watershed hydrological response to combined land use/land cover and climate change in highland Ethiopia: Finchaa catchment. *Water*, *12*(6), 1801.

ElNesr, M.N., Abu-Zreig, M.M., Alazba, A.A., 2010. Temperature trends and distribution in

the Arabian Peninsula. American Journal of Environmental Sciences 6, 191–203.

Fooladi, M., Golmohammadi, M. H., Safavi, H. R., Mirghafari, R., & Akbari, H. (2021). Trend analysis of hydrological and water quality variables to detect anthropogenic effects and climate variability on a river basin scale: A case study of Iran. *Journal of hydro-environment research*, *34*, 11-23.

Gaponov, V. M., Elizaryev, A. N., Aksenov, S. G., & Longobardi, A. (2019, November). Analysis of trends in annual time series of precipitation in the Republic of Bashkortostan, Russian Federation. In *IOP Conference Series: Earth and Environmental Science* (Vol. 350, No. 1, p. 012003). IOP Publishing.

Garg, V., Nikam, B. R., Thakur, P. K., Aggarwal, S. P., Gupta, P. K., & Srivastav, S. K. (2019). Human-induced land use land cover change and its impact on hydrology. *HydroResearch*, *1*, 48-56.

Gatgash, Z. E., & Sadeghi, S. H. (2024). Comparative effect of conventional and adaptive management approaches on watershed health. *Soil and Tillage Research*, *235*, 105869.

Gholizadeh Sarabi, S., Davary, K., Ghahraman, B., & Shafiei, M. (2021). A perceptual socio-hydrological model of co-evolutionary coupled human–water system based on historical analysis, Mashhad basin, Iran. *Hydrological Sciences Journal*, *66*(3), 355-372.

Giglou, A. N., Nazari, R., Karimi, M., Museru, M. L., Opare, K. N., & Nikoo, M. R. (2024). Future eco-hydrological dynamics: Urbanization and climate change effects in a changing landscape: A case study of Birmingham's river basin. Journal of Cleaner Production, 447, 141320.

Gocic, M., & Trajkovic, S. (2013). Trend analysis of water quality parameters for the Nisava river. *Facta universitatis-series: Architecture and Civil Engineering*, *11*(3), 199-210.

Guo, M., Lu, X., & Ma, Q. (2024). Assessment of Watershed Governance from an Ecological-Socioeconomic Perspective: A Case Study of the Liaohe River, China.

Herrmann, S.M., Brandt, M., Rasmussen, K. et al. 2020.Accelerating land cover change in West Africa over four decades as population pressure increased. Commun Earth Environ 1, 53. https://doi.org/10.1038/s43247-020-00053-y

Ishak, E. H., Rahman, A., Westra, S., Sharma, A., & Kuczera, G. (2013). Evaluating the non-stationarity of Australian annual maximum flood. *Journal of Hydrology*, *494*, 134-145.

Islam, S., Ojasvi, P. R., Srivastava, P., Gupta, A. K., & Yadav, R. S. (2020). Temperature and rainfall trend analysis at monthly scale in Dehradun District, Uttarakhand using variance corrected Mann-Kendall test. *Climate Change and Environmental Sustainability*, *8*(2), 201-212.

Izzati, U., Hasibuan, H. S. & Indra, T. L. (2019). Land Use change of Cisadane River Buffer Strips, South Tangerang city, IndonesiaIn proceeding of 13th Conference Southeast Asian Geography Association (SEAGA), 338(01), doi:10.1088/1755-1315/338/1/012019.

Kendall, M.G., Stuart, A., 1968. The Advanced Theory of Statistics: Design and Analysis, and Time-series, vol. 3. Charles Griffin & Company Limited, London.

Kim J, Choi J, Choi C, Park S (2013) Impacts of changes in climate and land use/land cover under IPCC RCP scenarios on streamflow in the Hoeya River basin, Korea. Sci Total Environ 452–453:181–195.

Kousari MR, Ahani H, Hendi-zadeh R (2013) Temporal and spatial trend detection of maximum air temperature in Iran during 1960–2005. Glob Planet Chang 111:97–110.

Kumar, M., Denis, D. M., Kundu, A., Joshi, N., & Suryavanshi, S. (2022). Understanding land use/land cover and climate change impacts on hydrological components of Usri watershed, India. *Applied Water Science*, *12*(3), 39.

Li, Z., Chen, X., Qi, J., Xu, C., An, J., & Chen, J. (2023). Accuracy assessment of land cover products in China from 2000 to 2020. Scientific Reports, 13(1), 12936.

Liu, Y. Y., Dorigo, W. A., Parinussa, R. M., de Jeu, R. A., Wagner, W., McCabe, M. F., ... & Van Dijk, A. I. J. M. (2012). Trend-preserving blending of passive and active microwave soil moisture retrievals. *Remote sensing of environment*, *123*, 280-297.

Liu, Y., Liu, F., Chen, C., Chen, Q., Zhang, J., Mo, K., ... & Yao, S. (2024). A holistic approach to projecting streamflow and analyzing changes in ecologically relevant hydrological indicators under climate and land use/cover change. Journal of Hydrology, 632, 130863.

López-Moreno, J. I., El Kenawy, A. M., Revuelto, J., Azorín-Molina, C., Morán-Tejeda, E., Lorenzo-Lacruz, J., ... & Vicente Serrano, S. M. (2014). Observed trends and future projections for winter warm events in the Ebro basin, northeast Iberian Peninsula.

Malede, D. A., Agumassie, T. A., Kosgei, J. R., Linh, N. T. T., & Andualem, T. G. (2022). Analysis of rainfall and streamflow trend and variability over Birr River watershed, Abbay basin, Ethiopia. Environmental Challenges, 7, 100528.

Mallakpour, I., & Villarini, G. (2015). The changing nature of flooding across the central United States. *Nature Climate Change*, *5*(3), 250-254.

Mann, H.B., 1945. Nonparametric tests against trend. Econometrica 13, 245‑259.

Mathews, R. and Richter, B. D.: Application of the indicators of hydrologic alteration software in environmental, Management of environmental flows, Freshwater Biol., 55, 194–205, https://doi.org/10.1111/j.1365-2427. 2009.02272.x, 2010.

Mekonnen, D, Duan, Z, Rientjes, T, Disse, M, 2018. Analysis of com117 0 bined and isolated effects of land-use and land-cover changes and 1171 climate change on the upper Blue Nile River basin's streamflow. Hy117 2 drology and Earth System Sciences 22 (12), 6187–6207. doi:10.5194/ 117 3 hess- 22- 6187- 2018.

Mishra AK, Ozger M, Singh VP (2009) Trend and persistence of precipitation under climate change scenarios for Kansabati basin, India. Hydrol Process 23:2345–2357.

Morid, R., Delavar, M., Eagderi, S., & Kumar, L. (2016). Assessment of climate change impacts on river hydrology and habitat suitability of Oxynoemacheilus bergianus. Case study: Kordan River, Iran. *Hydrobiologia*, *771*, 83-100.

Mostafazadeh, R., Zabihi Silabi, M., Azizi Mobaser, J., & Moezzipour, B. (2024). Index-based alteration of long-term river flow regimes influenced by land use change and dam regulation. Earth, 5(3), 404-419.

Nazeri Tahroudi, M., Ramezani, Y., & Ahmadi, F. (2019). Investigating the trend and time of precipitation and river flow rate changes in Lake Urmia basin, Iran. *Arabian Journal of Geosciences*, *12*, 1-13.

Niraula R, Meixner T, Norman LM (2015) Determining the importance of model calibration for forecasting absolute/relative

changes in streamflow from LULC and climate changes. J Hydrol 522:439–451.

Olden, J.D., Poff ,N.L. 2003. Redundancy and the choice of hydrologic indices for characterizing streamflow regimes. River Res Appl 19:101–121.

Pareeth, S., et al., 2019. Mapping agricultural landuse patterns from time series of Landsat 8 using random forest based hierarchial approach. Remote Sensing, 11 (5), 601. doi:10.3390/rs11050601.

Parizi, E., Hosseini, S. M., Ataie-Ashtiani, B., & Simmons, C. T. (2020). Normalized difference vegetation index as the dominant predicting factor of groundwater recharge in phreatic aquifers: case studies across Iran. *Scientific Reports*, *10*(1), 17473.

Praveen, B., Talukdar, S., Shahfahad, Mahato, S., Mondal, J., Sharma, P., ... & Rahman, A. (2020). Analyzing trend and forecasting of rainfall changes in India using non-parametrical and machine learning approaches. *Scientific reports*, *10*(1), 10342.

Puno RCC, Puno GR, Talisay BAM (2019) Hydrologic responses of watershed assessment to land cover and climate change using soil and water assessment tool model. Glob J Environ Sci Manag 5(1):71–82.

Richter, B. D., Baumgartner, J. V., Powell, J., & Braun, D. P. (1996). A method for assessing hydrologic alteration within ecosystems. *Conservation biology*, *10*(4), 1163-1174.

Saboohi R, Soltani S, Khodagholi M (2012) Trend analysis of temperature parameters in Iran. Theor Appl Climatol 109(3–4):529–547.

Sajid, M. (2022). Impact of land-use change on agricultural production & accuracy assessment through confusion Matrix. *Pakistan Journal of Science*, *74*(4).

Sen, P.K., 1968. Estimates of the regression coefficient based on Kendall's tau. Journal of the American Statistical Association 63, 1379–1389.

Shiau, J.-T. & Wu, F.-C. A Histogram Matching Approach for assessment of flow regime alteration: application to environmental flow optimization. River Research and Applications. 24, 914‑928 (2008).

Suryavanshi, S, Pandey, A., Chaube, UC (2017) Hydrological simulation of the Betwa river basin (India) using the SWAT model. Hydrol Sci J 62(6):960–978.

Tabari H, Talaee PH (2011) Recent trends of mean maximum and minimum air temperatures in the western half of Iran. Meteorog Atmos Phys 111(3–4):121–131.

Tabari, H., Marofi, S., 2011. Changes of pan evaporation in the west of Iran. Water Resources Management 25, 97–111.

Tadese, M., Kumar, L., Koech, R., & Kogo, B. K. (2020). Mapping of land-use/land-cover changes and its dynamics in Awash River Basin using remote sensing and GIS. *Remote Sensing Applications: Society and Environment*, *19*, 100352.

The Nature Conservancy (2009) Indicators of hydrological alteration version 7.1 user's manual.http://www.conservationgateway.org/ConservationPractices/Freshwater/EnvironmentalFlows/MethodsandTools/IndicatorsofHydrologicAlteration/Pages/IHA-Software-Download.aspx.

Torabi Haghighi, A., Darabi, H., Shahedi, K., Solaimani, K., & Kløve, B. (2020). A scenario-based approach for assessing the hydrological impacts of land use and climate change in the Marboreh Watershed, Iran. *Environmental Modeling & Assessment*, *25*(1), 41-57.

Villarini, G., & Smith, J. A. (2010). Flood peak distributions for the eastern United States. *Water Resources Research*, *46*(6).

Villarini, G., Serinaldi, F., Smith, J. A., & Krajewski, W. F. (2009). On the stationarity of annual flood peaks in the continental United States during the 20th century. *Water Resources Research*, *45*(8).

Wang G, Yang H, Wang L, Xu Z, Xue B (2014a) Using the SWAT model to assess impacts of land use changes on runoff generation in headwaters. Hydrol Process 28(3):1032–1042.

Wang R, Kalin L, Kuang W, Tian H (2014b) Individual and combined effects of land use/cover and climate change on Wolf Bay watershed streamflow in southern Alabama. Hydrol Process 28:5530–5546.

Wang, J., Li, J., Liu, S., Li, H., Chen, X., Peng, C., ... & Liu, X. (2021). Distinct microplastic distributions in soils of different land-use types: a case study of Chinese farmlands. *Environmental Pollution*, *269*, 116199.

Wang, X., Yang, T., Wortmann, M., Shi, P., Hattermann, F., Lobanova, A., & Aich, V. (2017). Analysis of multi-dimensional hydrological alterations under climate change for four major river basins in different climate zones. *Climatic Change*, *141*, 483-498.

Wood P.J., Agnew M.D., Petts G.E. (2000). Flow variations and macroinvertebrate community responses in a small groundwater-dominated stream in south-east England. Hydrol Process 14:3133–3147.

Xiong, J., & Yang, Y. (2024). Climate change and hydrological extremes. Current Climate Change Reports, 11(1), 1.

Xu, Z., Liu, Z., Fu, G., & Chen, Y. (2010). Trends of major hydroclimatic variables in the Tarim River basin during the past 50 years. Journal of arid Environments, 74(2), 256-267.

Yan, R., Gao, J., & Li, L. (2016). Modeling the hydrological effects of climate and land use/cover changes in Chinese lowland polder using an improved WALRUS model. Hydrology Research. https:// doi.org/10.2166/ hydro.2016.204.

Yan, Y., Yang, Z., Liu, Q. and Sun, T. (2010). Assessing effects of dam operation on flow regimes in the lower Yellow River. Procedia Environmental Sciences, 2, pp. 507-516. https://doi.org/10.1016/j.proenv.2010.10.055.

Yang, P., Yin, X.-A., Yang, Z.-F. & Tang, J. A revised range of variability approach considering the periodicity of hydrological indicators. Hydrological Processes. 28, 6222‑6235 (2014).

Yang, T., Cui, T., Xu, C. Y., Ciais, P., & Shi, P. (2017). Development of a new IHA method for impact assessment of climate change on flow regime. *Global and planetary change*, *156*, 68-79.

Yin J, He F, Xiong YJ, Qiu GY (2017) Effects of land use/land cover and climate change on surface runoff in a semi-humid and semiarid transition zone in northwest China. Hydrol. Earth Syst. Sci. 21:183–196.

Yonaba, R., Biaou, A. C., Koïta, M., Tazen, F., Mounirou, L. A., Zouré, C. O., ... & Yacouba, H. (2021). A dynamic land use/land cover input helps in picturing the Sahelian paradox: Assessing variability and attribution of changes in surface runoff in a Sahelian watershed. Science of the Total Environment, 757, 143792.

Yong, M., Shinoda, M., Nandintsetseg, B., Bi, L., Gao, H., & Wang, Y. (2021). Impacts of land surface conditions and land use on dust events in the inner Mongolian grasslands, China. *Frontiers in Ecology and Evolution*, *9*, 664900.

Zarenistanak M, Dhorde AG, Kripalani R (2014) Temperature analysis over southwest Iran: trends and projections. Theor Appl Climatol 116(1–2):103–117.

Zhang R, Xu Z, Zuo D, Ban C (2020) Hydro-meteorological trends in the Yarlung Zangbo River Basin and possible associations with large-scale circulation. Water 12(1):144. https://doi.org/10.3390/ w12010144.

Zhang, WX, Zhou TJ (2020) Increasing impacts from extreme precipitation on population over China with global warming. Sci Bull 65:243–252.

Zhang, T., Yan, T., Li, H., An, M., Du, X., Lei, Q., & Liu, H. (2025). Assessing climate change impact on watershed hydrological processes and stream temperature by considering CO2 emissions. *Water Research*, *286*, 124161.

Zhou, X., Huang, X., Zhao, H., & Ma, K. (2020). Development of a revised method for indicators of hydrologic alteration for analyzing the cumulative impacts of cascading reservoirs on flow regime. Hydrology and Earth System Sciences, 24(8), 4091-4107.

Frimpong, B. F., Koranteng, A., & Molkenthin, F. (2022). Analysis of temperature variability utilising Mann–Kendall and Sen's slope estimator tests in the Accra and Kumasi Metropolises in Ghana. Environmental Systems Research, 11(1), 2